

Temperature Effects on the Nonlinear Optical and Luminescence Properties for TCOs Based on In_2O_3 Layers Grown by Spray Pyrolysis

Zouhair Sofiani, Mohamed El Jouad, Souad khannyra

Laboratoire Optoélectronique et Physico-Chimie des Matériaux,
Université Ibn Tofail,
Faculté des Sciences BP 133 Kenitra 14000, Maroc

Abstract: Tin doped indium oxide thin films $\text{In}_2\text{O}_3\text{-Sn}$, have been deposited on glass substrate at various temperatures (450°C, 475°C, and 500°C), using spray pyrolysis techniques. The optimal substrate temperature to obtain films of high crystallographic quality was 500°C. For this temperature, the electrical resistivity is in the order of $3.10^{-4} \Omega\cdot\text{cm}$ and the average optical transmission in the visible region is larger than 95 %. The films were polycrystalline, crystallize in a cubic structure of the bixbyite Mn_2O_3 (I) type, and are preferentially orientated along the (400) direction. The cathodoluminescence spectra of $\text{In}_2\text{O}_3\text{-Sn}$ thin films taken at room temperature, present two emission peaks, the first one at 410 nm corresponding to indirect band gap emission and the second one at 650 nm is related to oxygen deficiencies acting as defects.

Keywords: Indium tin oxide, cathodoluminescence, Spray pyrolysis, Nonlinear optical properties

1. INTRODUCTION

Tin-doped indium oxide (ITO) thin films are being extensively studied because of the interesting properties they could have, such as a low resistivity, transparency in the visible region of the electromagnetic spectrum and high infrared reflectivity. These properties make them good candidates for many applications such as infrared reflectors, antireflection coatings, thin film resistors [1], heat reflecting mirrors for glass windows [2], photovoltaic devices [3], biological systems [4] and in a variety of electro-optical devices such as flat panel display devices [5,6]. Several methods have been used to get ITO films: reactive evaporation [7], the spray pyrolysis [8], chemical vapor deposition (CVD) [9], dc and RF magnetron sputtering [10,11] and last but not least sol-gel method.

In this work, we use spray pyrolysis technique, which is successfully used for transparent semiconducting film such as ZnO [12-14] and ZnS [15-17]. This technique is simple, cheap, easily adaptable if doping is required and allows large area deposition, this latter possibility being especially useful for the coating of windows in commercial buildings. Although some papers dealing with the physical properties of ITO obtained by spray pyrolysis technique (SP) have been published [18, 19, 20], the investigation of their luminescence remains very limited. The properties of sprayed ITO films are strongly dependent on the preparation conditions [21-23]. It is also shown that SP is an adapted technique to achieve ITO films with a quality comparable with that of transparent conducting oxide thin films prepared by other techniques [19, 24-30]. A careful control of the substrate temperature, the flow rate of the sprayed solution, the nozzle-substrate distance, the films thickness, and the concentration of dopant, is necessary to obtain the desired properties of coating for energy efficient windows.

2. EXPERIMENTAL DETAILS

The spray pyrolysis experimental set-up and the details on the procedure applied for the deposition of the investigated ITO thin films has been described elsewhere [31]. Tin-doped indium oxide thin films were prepared by spraying an alcoholic solution containing indium chloride InCl_3 and tin chloride $\text{SnCl}_2 \cdot 2\text{H}_2\text{O}$ used as dopant, on glass substrates heated from the backside by a ceramic heater at different temperatures (450°C, 475°C, and 500°C). The nozzle is directed towards the substrate

(distance nozzle-substrate = 0.45 m) and the spraying flow rate is set to 3.5 ml/min. All films have a thickness of 0.3 μm as estimated from the deposition time. The structural aspects were investigated by X-ray diffraction using Cu ($\text{K}\alpha$) radiation. Optical transmittance measurements were performed with a Shimadzu 3101 PC UV-VIS-NIR spectrophotometer, the analysis being extended to $\lambda = 2000$ nm. The cathodoluminescence set used was a home-made system that we have developed to perform near-field cathodoluminescence microscopy [32]. This one is based on the combination of a Scanning Force Microscope (SFM) and a Field Emission Scanning Electron Microscope (FESEM GEMINI 982 from LEO), the mechanical details of which are reported in Ref. [32]. The CL spectra were from well-defined spots of the sample, with a fixed electron beam at low accelerating voltage (5 kV). The photons were collected with a multimode optical fiber (NA=0.48) placed close to the sample surface (= 50 μm) and analyzed with a spectrometer that had a spectral resolution of 0.5 nm and was equipped with an N₂-cooled CCD detector. All spectra were acquired at room temperature. Third order nonlinear optical susceptibility $\chi^{(3)}$ of undoped and doped ZnO thin films was examined by THG technique (Figure. 1).

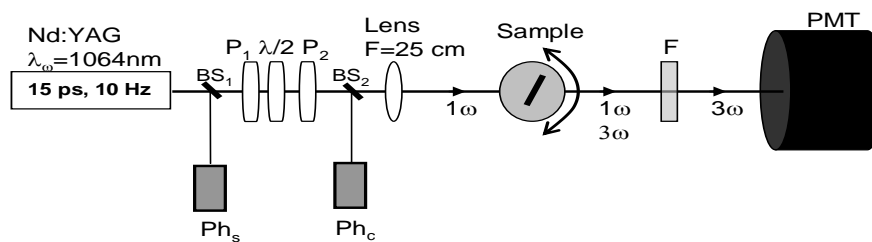


Fig1. THG experimental setup; Ph_s : synchronization photodiode; Ph_c : control photodiode; $\lambda/2$: half wave plate; BS: beam splitter; P: polarizer; F: transmitting filter at 355 nm, PMT: photomultiplier tube.

3. RESULTS AND DISCUSSION

The X-ray diffraction patterns of ITO films as a function of the substrate temperature are shown on Figure 2. The ITO thin films are polycrystalline and crystallize in a cubic structure of the bixbyite Mn_2O_3 (I) type (also called the c-type rare-earth oxide structure), since (222) and (400) oriented peaks, characteristic of a cubic structure, are present on the diffractograms. The preferred growth orientation of ITO thin films depends on the substrate temperature. The intensity ratio of the (400) to (222) reflection is used to evaluate the temperature effect on the film texture (table 1).

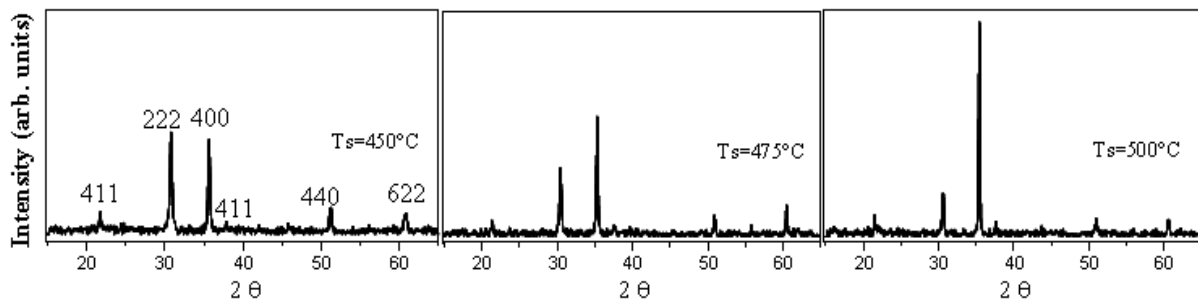


Fig2. X-ray pattern of In_2O_3 -Sn films (Sn concentration: 5 at. %) prepared at various substrate temperature: 450°C, 475°C and 500°

Table1. Ratio I_{400}/I_{222} and grain size of (222) and (400) peak at different substrate temperatures

Substrate temperature (°C)	450	475	500
I_{400}/I_{222}	1	1.75	5
Mean grain size of the (222) peak (nm)	27	32	32
Mean grain size of the (400) peak (nm)	31	37.5	45.4

The ratio I_{400}/I_{222} increases with increasing temperature, leading at 500°C to a clear predominance

of the (400) peak. Others peaks ((411); (622); (440)) are also observed, but their intensity is very small compared to that of the (400) peak. Nevertheless, their presence indicate that others orientations are possible on the films and that these orientations do not disappear with increasing temperature. To conclude, the films deposited at $T_s = 500^\circ\text{C}$ are polycrystalline with a preferential orientation along (400) plans. Note also that no characteristic peaks of impurity and dopant phases have been observed. The mean crystallite size D was calculated from the (400) and (222) diffraction peaks using Debye-Scheerer's formula (1):

$$D = \frac{K\lambda}{\Delta(2\theta)\cos(\theta)} \quad (1)$$

In which is the X-ray wavelength (1.548 \AA for $\text{Cu}(K\alpha)$), $K = 180/\pi$, θ is the diffraction angle and $\Delta(2\theta)$ is the full line-width at half maximum of the (400) and (222) peaks. The line-widths were measured at a narrow slit width for better resolution (spectra not shown). The measured line-widths and the corresponding mean crystallite sizes are regrouped on table 1. The mean size increases slowly with increasing temperature for the (222) oriented crystallites, keeping around approximately 30 nm, whereas the rise is important and continuous for the (400) oriented crystallites. So, a partial healing of the film is observed with increasing substrate temperature, accompanied by a size increase of the (400) oriented grains. Typical SEM images, of the surfaces of the ITO films deposited at different substrate temperatures are shown on Figure 3. Note that no cracks are observed on large scan area for all samples. The films are continuous and in fact consist of grains.

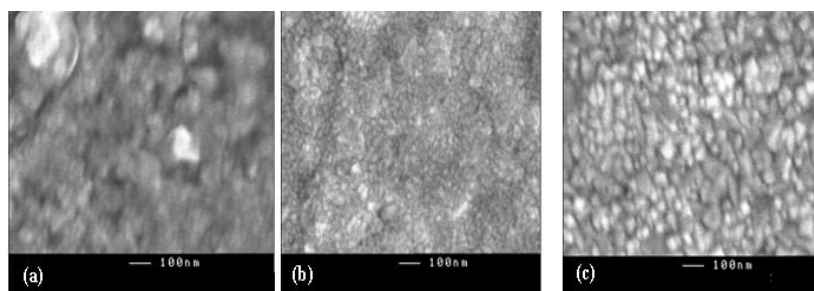


Fig3. SEM images of $\text{In}_2\text{O}_3\text{-Sn}$ films (Sn concentration: 5 at. %) prepared at different substrate temperature: 450°C , 475°C and 500°C

At $T_s = 450^\circ\text{C}$, the film appears very smooth containing large grains. At $T_s = 475^\circ\text{C}$, the large grains seem to disappear and very small particles appear. The process of re-crystallization is achieved at $T_s = 500^\circ\text{C}$, and the surface is entirely covered by grains with a narrow size distribution. The XRD results are therefore confirmed by SEM imaging: the crystallization of ITO films increase with the substrate temperature. We can qualitatively explain these results by using the critical optimization concept described by P.S. Vincett [33] and J. Georges [34]. These authors observe that the films deposited at low temperatures are a mixture of crystallized and amorphous regions. At the boiling point of the substance, the amorphous regions vaporize during the film growth. Furthermore, the diffusion in the bulk becomes relatively important at the optimal temperature and contributes to the filling of the lacunas created by the evaporation of the disordered regions. Consequently, the crystallinity improves leading to well-ordered and well-oriented films.

Figure 4 shows the optical transmittance curves as a function of the wavelength for the ITO films deposited at various substrate temperatures. The films deposited at 500°C exhibit a high optical transmittance (greater than 90 %) in the visible region and high reflectance in the infrared one. The average optical transmittance and reflectance increase with the substrate temperature. The observed reflectance is due to a plasma effect resulting from the high concentration of free electrons in our thin films. Furthermore, the absorption edge shifts towards shorter wavelength, suggesting a widening of the energy band-gap with increasing substrate temperature. The shift in absorption edge, called the Brustein-Moss shift [35], was also reported by another group [36]. These features suggest that ITO films with enhanced optical properties can be produced by spray pyrolysis at $T_s = 500^\circ\text{C}$. We obtain, at higher substrate temperature, a window which is transparent for solar radiation, so that maximum benefit can be received from direct solar heating, while the thermal emittance is decreased thereby

improving the insulation and making the window a less serious heat leak. The desired properties of coatings for energy-efficient windows are therefore achieved.

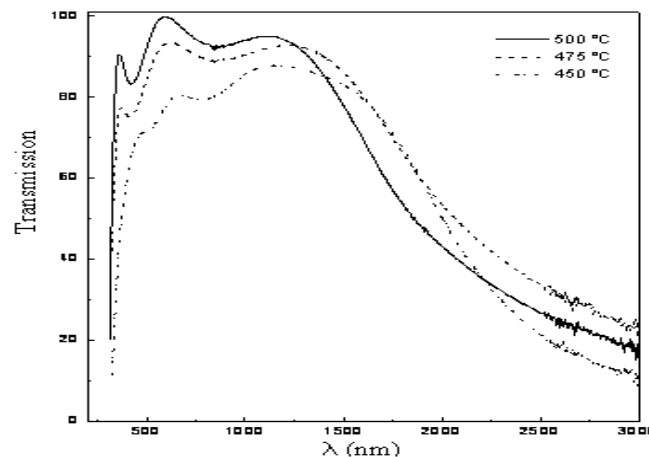


Fig4. Optical transmission of In_2O_3 -Sn films doped at 5 at. % Sn and prepared at different substrate temperature: 450°C, 475°C and 500°C

Figure 5 shows the cathodoluminescence emission spectra of our ITO thin films. The electron beam energy was 5 keV. All samples present two main emission peaks located at $\lambda = 410$ nm and $\lambda = 650$ nm. By focusing the electron beam on the fiber, we verified that our silica fiber did not emit at a wavelength near to 410 nm (spectrum not shown). So, the luminescence at 410 nm ($E_\lambda = 3.03$ eV) corresponds to a transition characteristic of ITO. For polycrystalline or amorphous ITO material, it is reported that light is absorbed by both direct and indirect band gap interband transition. A typical value of ITO optical direct band gap is 3.6 eV ($\lambda = 345$ nm), as reported in the literature [37]. It is also reported [38] that the direct band gap shifts from 3.7 eV to 4.2 eV when the carrier concentration increases from $3.2 \cdot 10^{19}$ to $8.23 \cdot 10^{20} \text{ cm}^{-3}$, and the indirect band gap shifts from about 2.8 eV to 3.4 eV when the carrier concentration increases from $5.38 \cdot 10^{19}$ to $6.54 \cdot 10^{20} \text{ cm}^{-3}$. Our emission at 410 nm corresponds therefore to an indirect band gap transition, with a carrier concentration calculated by hall effect is $4 \cdot 10^{20} \text{ cm}^{-3}$. As our optical fiber cut off the optical signal for wavelength lower than 330 nm, we do not observe the direct band gap emission which occurs between 330 nm (3.7 eV) and 295 nm (4.2 eV). This interpretation is confirmed by H. Rhaled and al. [39]. S. Laux and al. [40] also measure an indirect band gap of 2.97 eV and a direct band gap of 3.75 eV, for ITO thin films deposited by plasma ion-assisted evaporation.

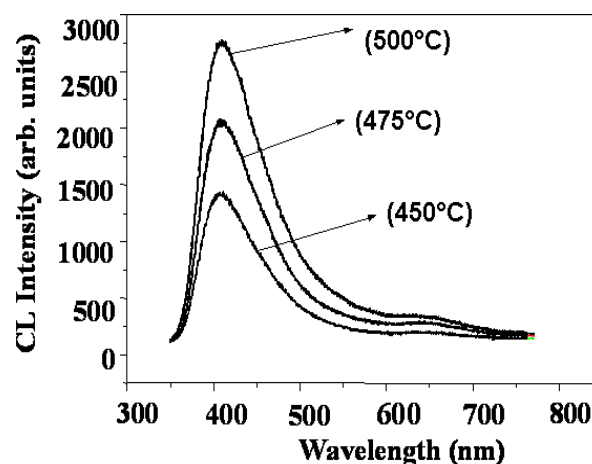


Fig5. Cathodoluminescent spectra of In_2O_3 -Sn films doped at 5 at. % Sn as a function of substrate temperature: 450°C, 475°C and 500°C

The second peak is the well-known orange emission ($E_\lambda = 1.9$ eV), probably due to oxygen deficiencies, acting as defects [41]. The CL intensity of all peaks increases with the substrate temperature, but the ratio CL intensity at $\lambda = 410$ nm on CL intensity at $\lambda = 650$ nm remains constant.

That implies that the density of oxygen deficiency doesn't change with substrate temperature. CL intensity is directly correlated to an improvement of the films crystallinity. Further, when the substrate temperature increases, the surface of our films is entirely covered by grains and dense (figure 3). The density of grain boundaries and dislocations decreases, leading to the enhancement of cathodoluminescence intensity of ITO thin films. ITO thin films deposited at 500° C presents a better Cathodoluminescence intensity (figure 5).

We also carried out a study of cathodoluminescence according to the various of Sn doping (2%, 5% and 10%) (figure 6).

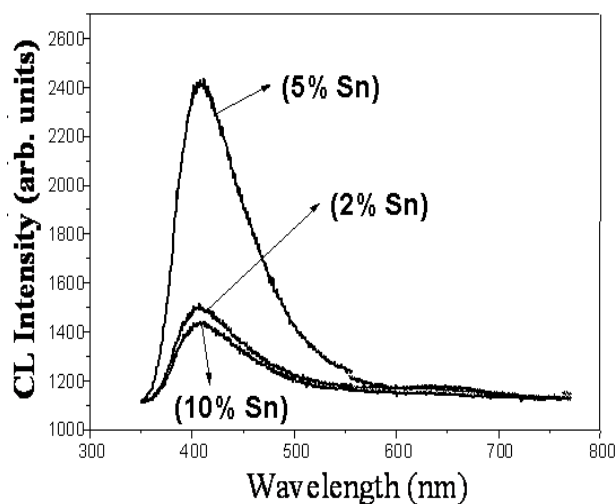


Fig6. Cathodoluminescent spectra versus Sn-dopant concentration of In_2O_3-Sn films deposited at 500°C: 2 at. % Sn, 5 at. % Sn and 10 at. % Sn.

The substrate temperature is fixed at 500°C. The spectra shows tow bands already announced and the cathodoluminescence intensity varied with doping concentration; an important intensity is manifested at 5 at. % Sn, corresponding to a cristallinity as we can see in figures 7 and 8.

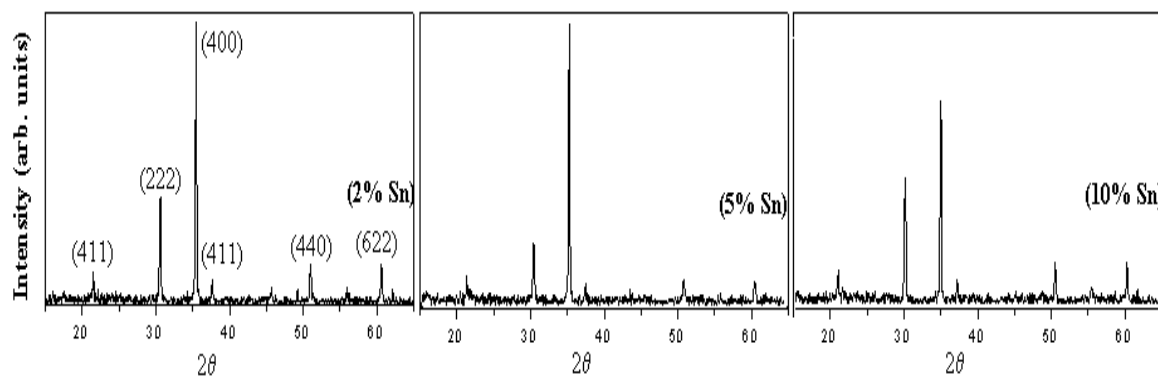


Fig7. XRD patterns of In_2O_3-Sn films deposited at 500°C versus Sn-dopant concentration: 2 at. % Sn, 5 at. % Sn and 10 at. % Sn.

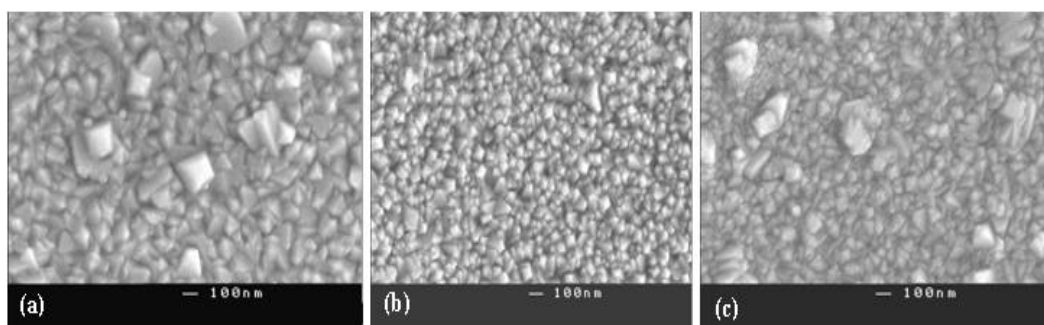


Fig8. SEM images of In_2O_3-Sn versus Sn-dopant concentration of In_2O_3-Sn films deposited at 500°C: 2 at. % Sn, 5 at. % Sn and 10 at. % Sn

Temperature Effects on the Nonlinear Optical and Luminescence Properties for TCOs Based on In_2O_3 Layers Grown by Spray Pyrolysis

The change in the preferential orientation from (222) to (400) peak may strongly depends on the Sn concentration. The change in the preferential orientation was well studied by many authors [42-45]. They attributed the modification of the preferred orientation from (222) to (400) to the existence of the quantities of oxygen atoms in the In_2O_3 matrix. Oxygen incorporation leads to (222) orientation, and (400) orientation is related to oxygen deficiency. To conclude, the 5% Sn doped film is polycrystalline with a preferential orientation along (400) plans. Note also that, no characteristic peaks of impurity and dopant phases have been observed.

The scanning electron microscopy (SEM) images of the IFO films formed at different Sn concentrations Fig. 2(a)–(c). The micrographs indicate that there is a change in the surface morphology of the films. The films are continuous and in fact consist of grains. At $T_s = 450^\circ\text{C}$, the film appears very smooth containing large grains. The surface is entirely covered by grains with a narrow size distribution at 5 at. % Sn which confirm by XRD patterns.

Figure 10 shows us the obtained results from the selected samples with different doping agent, we find the following values of the third nonlinear susceptibility $\chi(3)$:

$$\text{In}_2\text{O}_3:\text{Sn } 2\% \quad \chi(3) = 9.37 \cdot 10^{-11} \text{ esu}$$

$$\text{In}_2\text{O}_3:\text{Sn } 5\% \quad \chi(3) = 10.45 \cdot 10^{-11} \text{ esu}$$

$$\text{In}_2\text{O}_3:\text{Sn } 10\% \quad \chi(3) = 9.26 \cdot 10^{-11} \text{ esu}$$

We see that, the obtained values exhibit clearly the strong correlation which exist between the linear Optical and structural properties of the thin films with the nonlinear Optical properties. The growth parameters influence strongly the nonlinear properties. The ONL coefficient is mainly related to the surface interface and the crystallinity of the thin film. This is explained by the fact that light and matter interaction is related to the interface where the light comes and the contact surface should be so smooth and have a regular shape that enhance the interaction with light, thus can allow the light go trough to material and extract the property in the heart of the material.

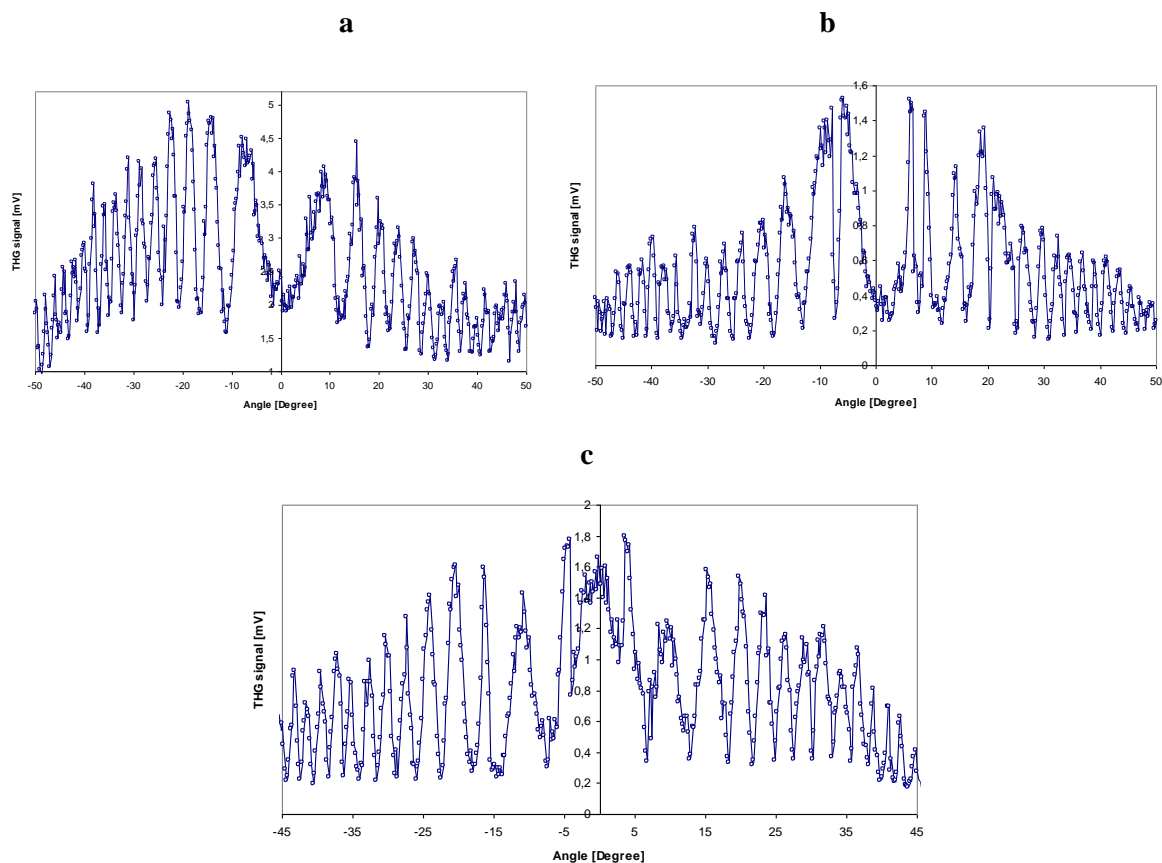


Fig11. Third Harmonic generation efficiency for In_2O_3 -Sn samples a: 2%, b: 5%, c: 10% and c: 10%.

Figure 10 shows us the obtained results from the selected samples with different doping agent, we find the following values of the third nonlinear susceptibility $\chi(3)$:

$$\text{In}_2\text{O}_3:\text{Sn } 2\% \quad \chi(3) = 9.37 \cdot 10^{-11} \text{ esu}$$

$$\text{In}_2\text{O}_3:\text{Sn } 5\% \quad \chi(3) = 10.45 \cdot 10^{-11} \text{ esu}$$

$$\text{In}_2\text{O}_3:\text{Sn } 10\% \quad \chi(3) = 9.26 \cdot 10^{-11} \text{ esu}$$

We see that, the obtained values exhibit clearly the strong correlation which exist between the linear Optical and structural properties of the thin films with the nonlinear Optical properties. The growth parameters influence strongly the nonlinear properties. The ONL coefficient is mainly related to the surface interface and the crystallinity of the thin film. This is explained by the fact that light and matter interaction is related to the interface where the light comes and the contact surface should be so smooth and have a regular and symmetric shape that enhance the interaction with light, thus can allow the light go trough to material and extract the property in the heart of the material.

Transparent and good crystalline films are strongly required to get higher nonlinear coefficients.

4. CONCLUSION

The effect of substrate temperature on the structural, optical and cathodoluminescence properties of spray-deposited Sn-doped In₂O₃ thin films has been reported in this paper. The 5% Sn doped film deposited at 500°C are polycrystalline and exhibit a preferential orientation along the (400) direction. A good visible transmittance of about 90-95 % were obtained for this sample. The cathodoluminescence spectra presents two emission bands that do not depend on the substrate temperature: a first one centered at $\lambda = 410$ nm, corresponding to indirect band gap emission, and a second one at $\lambda = 650$ nm, the so-called orange emission, associated to oxygen deficiencies. The film at 5% Sn presents a better cathodoluminescence intensity, have the good crystallinity. To conclude, it seems that the cathodoluminescence intensity enhances with the film have a good crystallinity and good transmittance. In addition we find that, the nonlinear optical properties are enhanced by having a good surface morphology, good transparent films as well as a better crystallinity. The film with 5% at. of Sn doped In₂O₃ exhibits the higher value of the third harmonic signal, which correlates with the same obtained results.

REFERENCES

- [1] R. B. Tahar, T. Ban, Y. Ohya, Y. Takahashi, J. Appl. Phys., 83, 2631 (1998).
- [2] K.L. Chopra, S.R. Das, Thin Film Solar Cell, Plenum Press, New York 1983, p. 321.
- [3] C.V.R. Vasant Kumar, A.A. Mansingh, J. Appl. Phys. 65 (1989) 1270.
- [4] L. Tamisier, A. Carani, Electrochim. Acta 32 (1987) 1365.
- [5] J.E. Costellamo, Handbook of Display Technology, Academic Press, New York 1992.
- [6] S. Ishibashi, Y. Higushi, Y. Ota, K. Nakamuva, J. Vac. Sci. Technol. B 18 (1990) 1399.
- [7] S. Kasiwiswnathan, V. Srinivas, A. K. Kar, B. K. Matur, K. L. Chopra, Solid State Comm., 101, 831 (1997).
- [8] H. Kobayashi, S. Tachibana, K. Yamanaka, Y. Nakato, K. Yoneda, J. Appl. Phys., 81, 7630 (1997).
- [9] T. Maruyama, K. Tabana, Jpn. J. Appl. Phys. , 29, L355 (1990).
- [10] C. Hoon Yi, I. Yasui, Y. Shigesato, Jpn. J. Appl. Phys., 34, L244 (1995).
- [11] M. C. de Andrade, S. Moehlecke, Appl. Phys. A 58, 503 (1994).
- [12] A. El Hichou, A. Bougrine, J.L. Bubendorff, J. Ebothe, M. Addou, M. Troyon , Semiconductor Science and Technology B, 17 (2002) 607.
- [13] S. A. Studenikin, N. Golego, M. Cocivera, J. Appl. Phys. 83 (1998) 2104.
- [14] F. Paraguay, D. J. Morales, W. Estrada, L. E. Andrade, M. Miki-Yoshida Thin Solid Films, 366 (2000) 16.
- [15] B. El Idrissi, M. Addou, A. Outzourit, M. Regragui, A. Bougrine, A. Kachouane, Solar Energy Materials and Solar Cells 69 (2001) 1.

- [16] A. Ortiz, J. Alonso, V. Pankov, J. Mater. Sci. 10 (1999) 503.
- [17] K. T. R. Reddy, H. Gopalasswamy, P. J. Reddy, R. W. Miles, J. Cryst. Grow. 210 (2000) 516.
- [18] E. Benamar, M. Rami, C. Messoudi, D Sayah, A. Enaoui, Solar Energy Materials and Solar Cells 56 (1999) 125.
- [19] H. Bisht, H. T. Eun, A. Mehrrens, M. A. Aegerter, Thin Solid Films 351 (1999) 109.
- [20] Z.B. Zhou, R.Q. Cui, Q.J. Pang, Y.D. Wang, F.Y. Meng, T.T. Sun, Z.M. Ding, X.B. Yu, Appl. Surface Sci. 172 (2001) 245.
- [21] C.H. Yi, Y. Shigesato, I. Yasui, S. Takaki, Jpn. J. Appl. Phys. 34 (1995) L244.
- [22] T.J. Vink, W : Walrave, J.L.C. Daams, P.C. Baarslag, J.E.A.M. Van der Meerakker, Thin Solid Films 266 (1995) 145.
- [23] P.K. Song, Y. Shigesato, I. Yasui, C.W. Ow-Yang, D.C. Paine, Jpn. J. Appl. Phys. 37 (1998) 1870.
- [24] A. Kachouane, M. Addou, A. Bougrine, B. El Idrissi, R. Messoussi, M. Regragui, J. C. Bérned, Materials Chemistry and Physics 70(3) (2001) 285.
- [25] M. Kamei, Y. Shigesato and S. Takaki, Thin Solid Films 259 (1995) 38.
- [26] A. K. Kulkarni, Kirk H. Schulz, T. S. Lim, M. Khan, Thin Solid Films 345 (1999) 273.
- [27] S. H. Shin, J. H. Shin, K. J. Park, T. Ishida, O. Tabata, H. H. Kim, Thin Solid Films 341 (1999) 225.
- [28] P. Thilakan, S. Kalainathan, J. Kumar, P. Ramasamy, J. Electron. Mater. 24 (1995) 719.
- [29] S. Mizapour, S.M. Rozatis, M.G. Takwale, B.R. Marathe, V.G. Vhide, Mater. Res. Bull. 27 (1992) 1992.
- [30] C.H. Lee, C.S. Huang, Mater. Sci. Eng. (Solid State Mater Adv. Technol) 22 (1994) 233.
- [31] M Addou, A.Moumin, B. Elidrissi, M Regragui, A.Bougrine, A.Kachouane and C. Monty, J. Chem. Phys 96(2) (1999) 232.
- [32] M. Troyon, D. Pastre, J. P. Jouart, J. L. Beaudoin, Ultra-microscopy 75 (1998) 15.
- [33] P.S. Vincett, Thin Solid Films 100 (1983) 371.
- [34] J. George, K.S. Joseph, B. Pradeep, T.I. Palson, Phys. Stat. Sol. A 106 (1988) 123.
- [35] E. Burstein, Phys. Rev. 93 (1952) 632.
- [36] I. Hamberg, C.G.Granqvist, J. Appl. Phys. 60 (1986) R123.
- [37] M. Penza, S. Cozzi, M. A. Tagliente, L. Mirengi, C. Martucci, A. Quirini, Thin Solid Films 349 (1999) 71.
- [38] Y. Ohhata, F. Shinoki, S. Yoshida, Thin Solid Films 59 (1979) 255.
- [39] H. El Rhaleb, E. Benamar, M. Rami, J. P. Roger, A. Hakam, A. Ennaoui, Appl. Surf. Sci., 201 (2002) 138.
- [40] S. Laux, N. Kaiser, A. Zöllner, R. Götzelmann, H. Lauth, H. Bernitzki, Thin Solid Films, 335 (1998) 1.
- [41] Min-Suk Lee, Won Chel Choi, Eun Kyu Kim, Chun Keun Kim and Suk-Ki Min, Thin Solid Films 279 (1996) 1.
- [42] S. Parthiban, V.Gokulakrishnan, K.Ramamurthi, E.Elangovan, R.Martins, E. Fortunato, R.Ganesan, Solar Energy Materials & Solar Cells 93, 92–97 (2009).
- [43] T. Koida, M. Kondo, J. Appl. Phys. 99, 1237031–1237035 (2006).
- [44] L. J. Meng, M. P. dos Santos, Thin Solid Films 322, 56 (1998).
- [45] Bo. Zhang, Xianping Dong, Xiaofeng Xub and Jiansheng Wua, Scripta Materialia. 58, 203–206 (2008).

AUTHORS' BIOGRAPHY



Dr. Zouhair SOFIANI, Assistant Professor at Ibn Tofail University, Kenitra, Morocco since 2010. PhD from Angers University, Angers, France in 2007, on Photonics. http://www.researchgate.net/profile/Zouhir_Sofiani

Dr. Mohamed EL Jouad, Postdoctoral Researcher at Ibn Tofail University, Kenitra, Morocco since 2012. PhD from Angers University, Angers, France in 2010, on Photonics. http://www.researchgate.net/profile/Mohamed_El_jouad